

Received July 7, 2020, accepted August 7, 2020, date of publication August 25, 2020, date of current version September 9, 2020.

Digital Object Identifier 10.1109/ACCESS.2020.3019362

Derivation of Optimized Equations for Estimation of Dispersion Coefficient in Natural Streams Using Hybridized ANN With PSO and CSO Algorithms

HOSSIEH RIAHI MADVAR¹, MAJID DEGHANI², RASOUL MEMARZADEH², ELY SALWANA⁹, AMIR MOSAVI^{3,4,5,6,10}, AND SHAHAB S.^{7,8}, (Senior Member, IEEE)

¹Department of Water Science and Engineering, Faculty of Agriculture, Vali-e-Asr University of Rafsanjan, Rafsanjan 7718897111, Iran

²Department of Civil Engineering, Faculty of Technical and Engineering, Vali-e-Asr University of Rafsanjan, Rafsanjan 7718897111, Iran

³Kalman Kando Faculty of Electrical Engineering, Obuda University, 1034 Budapest, Hungary

⁴Thuringian Institute of Sustainability and Climate Protection, 07743 Jena, Germany

⁵Faculty of Civil Engineering, Technische Universität Dresden, 01069 Dresden, Germany

⁶Department of Informatics, J. Selye University, 94501 Komarno, Slovakia

⁷Institute of Research and Development, Duy Tan University, Da Nang 550000, Vietnam

⁸Future Technology Research Center, College of Future, National Yunlin University of Science and Technology, Yunlin 64002, Taiwan

⁹Institute of IR4.0, Universiti Kebangsaan Malaysia, Bangi 43600, Malaysia

¹⁰Norwegian University of Life Sciences, 1430 Ås, Norway

Corresponding authors: Amir Mosavi (amir.mosavi@kvk.uni-obuda.hu) and Shahab S. (shamshirbandshahaboddin@duytan.edu.vn)

This research is carried out as part of the EFOP-3.6.2-16-2017-00016 project in the framework of the New Szechenyi Plan. The completion of this project is funded by the European Union and co-financed by the European Social Fund. We acknowledge the financial support of the Hungarian State and the European Union under the EFOP-3.6.1-16-2016-00010 project and the 2017-1.3.1-VKE-2017-00025 project. This research has been additionally supported by the Project: ‘Support of research and development activities of the J. Selye University in the field of Digital Slovakia and creative industry’ of the Research & Innovation Operational Programme (ITMS code: NFP313010T504) co-funded by the European Regional Development Fund.

ABSTRACT In this paper, a new hybrid model is developed to improve the accuracy in the prediction of the longitudinal dispersion coefficient (K_L) and the derivation of novel optimized explicit equations for natural streams. For this purpose, an artificial neural network (ANN) is hybridized with particle swarm optimization (PSO) and cat swarm optimization (CSO) algorithms. The CSO and PSO are used to find the optimum values of biases and weights in ANN structure and formulate the results as novel explicit predictive equations than the classical black-box methods. The hydraulic parameters of the natural stream and some geometric parameters were utilized for the model developments. Eight different input combinations are used as the input vectors to ANN, ANN-PSO, and ANN-CSO models, whereas the dispersion coefficient (K_L) is the target model output. The developed models are trained and tested by a comprehensive reference data sets measured on streams in the United States, that were used previously by Tayfur and Singh (2005) in ANN models. The main aims, novelty, and contributions of the present study are 1) improving the accuracy of classical ANN-based K_L predictions by hybridizing with CSO and PSO. 2) Performing sensitive analysis of ANN, ANN-CSO, and ANN-PSO based on input combinations 3) derivation of novel explicit optimized ANN-CSO, ANN-PSO, equations for predicting K_L rather than the classical ANN black-box methods. The results depicted that the highest accuracy and superiority were attained by the ANN-PSO model, with input variables of B, H, U, U_* , followed by ANN-CSO and ANN. By using the optimized trained black box ANN models, two novel explicit predictive equations are derived, and their results are compared with the empirical equations. Comparative assessments confirmed significant improvements in the hybrid equations’ results than the classical ANN and previously published equations. The developed novel equations can be used to estimate the K_L in one-dimensional pollutant transfer models that are essential for the pollution studies in environmental river engineering practices.

INDEX TERMS Longitudinal dispersion coefficient, PSO, CSO, ANN, natural rivers, explicit equation derivation, streamflow, optimization.

I. INTRODUCTION

The associate editor coordinating the review of this manuscript and approving it for publication was Jenny Mahoney.

The study of pollutant and contaminant transport in the natural streams is important in several aspects such as quality

management, pollution control of the chemical and biological processes, hydro-ecological studies and environmental impact assessments [1], [2]. Hazardous pollutants and effluents, when discharged to the streams, in the mixing process, dispersed transversely, vertically, and longitudinally by advective and dispersive processes. At a distance downward from the source injection, the longitudinal dispersion becomes the essential mechanism and quantified by the longitudinal dispersion coefficient (K_x) [3]. K_x is a crucial factor in studying the environmental hydraulics of water quality in rivers [4], [5]. In applied aspects of river engineering such as pollutant transport, the dominant process is one-dimensional [6], and the longitudinal dispersion acts as the most crucial parameter in modeling the fate of contaminants chemicals, nutrients, sediments and river water quality [1], [7]–[9]. The longitudinal dispersion process as the primary mechanism in applied river quality studies is simulated by the conventional advection-dispersion equation [10]:

$$\frac{\partial C}{\partial t} + u \frac{\partial C}{\partial x} = K_x \frac{\partial^2 C}{\partial x^2} \quad (1)$$

where C is the average of mass concentration (mg/l) in cross-section, t is the time (s) in unsteady modeling, u is the longitudinal velocity (m/s), x is the longitudinal coordinate (m), and K_x is the longitudinal dispersion coefficient (m^2/s) [11]–[13]. It is possible to obtain K_x by solving the advection-diffusion equation [9]. Therefore, the development of the empirical-based formulas for the K_x in terms of the basic features of the rivers has been considered [14], [15]. For complex case studies such as the natural rivers with large transverse velocity shear, the dispersion coefficient estimation is time-consuming with a high level of uncertainties [10], [16]. According to the previous studies, the flow depth (H), section width (B), mean flow velocity (U), bed shear velocity (U_*), river shape parameter (b), channel sinuosity (s) in river sections and the combinations of them (e.g., the flow discharge, Q) are the most influential parameters for determination of the K_x [17]–[21]. Based on these hydraulic and hydrodynamic parameters, several researches were carried out to develop a formula for estimation of the K_x based on the following representation [5]:

$$K_x = f(H, B, U, u_*, b, \sigma, Q) \quad (2)$$

For this purpose, several methods including empirical/mathematical based equations [22]–[25], statistical and regression-based equations [14], [17], [26], [27] and in recent years different models of soft computing such as adaptive neuro fuzzy inference system (ANFIS), support vector machine (SVM), Gene expression programming (GEP) and ANN [3], [6], [9], [11], [12], [28]–[31] were used to predict and develop a formula that can be used in the estimation of K_x in natural rivers. Most of the recent studies discussed that new flexible structure-based models such as ANN outperformed the older rigid structure but simple models [11]–[13], [15]. Although artificial intelligence-based models showed superiorities in K_x estimation, yet, the main challenging problem

that limited their applicability is their black-box nature. Soft computing techniques work as a black-box model in which the process of a phenomenon is not considered in modeling, and the governing relationship is just based on the input-output data without providing explicit estimation equation [32], [33]. The ANN is the most widely used method in water resources modeling [4], [20], [34]–[36]. Multilayer perceptron (MLP) with a feed-forward back-propagation algorithm is one of the most popular types of ANN, which was used for forecasting hydrological variables such as drought, streamflow, evaporation, etc. [37]–[42]. The capability of ANN-based models in fast learning and using noisy data made them accessible during the past decades [43]. However, the same as other methods it has some shortcomings. Among all, as the procedure of training is based on finding the optimum solution as the best fit, it may trap in local instead of the global optimum. Another drawback in ANN models is operating at much slower speeds compared to the acceptable level and slow training algorithms such as gradient methods [20], [43]. The meta-heuristic optimization algorithms showed considerable achievements in previous studies and the literature reported great enhancement in model performances. Moreover, their hybridization with the ANN aimed to overcome the problem of local optimum and avoid local minima that convergence rates of heuristic methods to the global minimum can be faster than back propagation.

To remedy these problems, several optimization algorithms have been developed during the past decades. In recent years, nature-inspired optimization algorithms are proposed to find the global optimum in optimization problems. For estimation of the K_x , different optimization algorithms, including genetic algorithm (GA) [20], [28], [44]–[46], PSO [6], Differential Evolution (DE) [30], [44], and Genetic Programming (GP) [9], [31], [48], [11] were used. All of these studies come in with major drawbacks. The main drawback is their inapplicability for explicit future estimation of the K_x , without providing explicit equation based on the results. Nearly all of these studies are based on a black-box framework and based on the knowledge of the authors, there is no explicit optimized ANN-based equation for K_x estimation. On the other hand, in natural streams, the need and emphasis is on explicit estimation for the K_x , not on the black box models. Thus, further attempts are still vital to hybridize ANN models with more robust recent optimization techniques in order to result in an accurate, explicit equation for the estimation of longitudinal dispersion coefficient, especially for future use in one-dimensional water quality studies.

There is a need to develop objective procedures for the explicit derivation of new predictive equations based on optimized black-box models of ANN for longitudinal pollutant dispersion coefficient using multiple variables that affect the K_x values. This will be accomplished by the establishment of a hybridizing scheme that requests evidence from multiple sources of hydraulic, geometry, and shear force and will, therefore, empower better estimation of the K_x based on the inherent knowledge. This study directed to

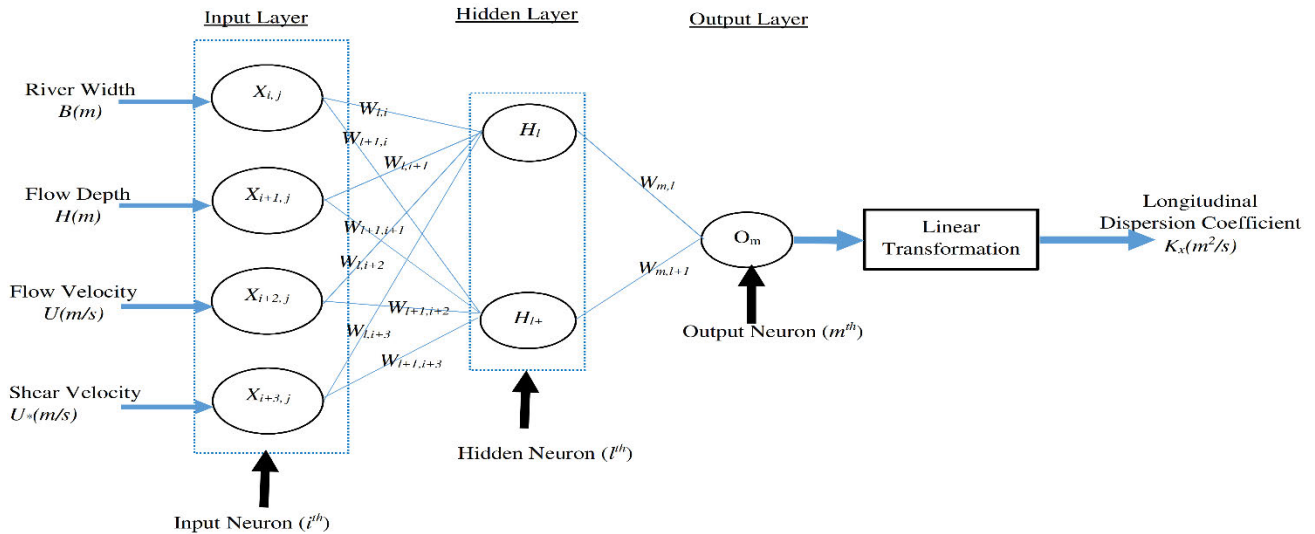


FIGURE 1. The ANN model structure for the prediction of K_x .

deal with the complex dependent interactions between various dispersion related parameters and generation of explicit prediction equations. To achieve this aim, CSO and PSO are used to train the ANN and derivation and amplifying of dependence structure of the K_x in equation-based forms. This will extend our knowledge into the applicability and white box status of ANN-based results than the black box results and improve our ability to illustrate them.

In this paper, motivated by the satisfactory performance of PSO and CSO algorithms, and to overcome the previously mentioned shortcomings, the ANN hybridized with CSO and PSO algorithms. Another main contribution of the present study is that for the first time, an explicit optimized-based equation for accurate determination of the longitudinal dispersion coefficient was developed. In this study, the authors proposed a new methodological framework for the derivation of explicit equations for the longitudinal pollutant dispersion coefficient using black-box models of hybrid ANN that empowers us to compute an intelligence-based K_x . Also, the traditional ANN was used for modeling, and the improvements in the results are compared with the hybrid models and previous results of ANN in Tayfur and Singh (2005) study and previous empirical equations. The database used in this research is a worldwide-accepted real dataset in studies of K_x over natural rivers provided in Tayfur and Singh (2005). Training and testing of models are accomplished using this dataset, and the obtained results of different models with various input parameters are evaluated by virtue of several graphical and statistical indices. In the final step of the current study, two explicit predictive equations are provided, and a comparison is drawn between developed equations with some well-known empirical equation of K_x .

The major contributions and novelty of the developed framework in this study are summarized as follows:

- In the current study, a novel hybrid algorithm for training ANN entitled ANN-CSO, is developed and its performance is evaluated with ANN-PSO and stand-alone ANN.
- The developed hybrid models of ANN-PSO, ANN-CSO are used to provide two explicit predictive equations for K_x via an optimal solution.
- Development of a new methodological framework for equation derivation based on ANN optimized models that empower us to use the results of ANN-based models in other studies.

The remainder of the paper is organized as follows. At first, an overview of the ANN, PSO, CSO are presented. After that, an explanation of the collected data and train-test subsets are provided and previously published equations for K_x estimation are presented. Then modeling hybridization framework also included with evaluation criteria, and finally, the application results, discussion, and conclusions of the study with recommendations for future are provided.

II. MATERIAL AND METHODS

A. ARTIFICIAL NEURAL NETWORKS

Artificial neural network (ANN) widely used in water resources researches during the past decades. The multi-layer perceptron (MLP) has three or more layers, including input, one or more hidden, and one output layers. The output is generated from the summation of the weights from the preceding layer in a node, adding bias and deriving the output through a transfer function [40]. ANN as a black-box model, with a non-linear relationship between the input and output parameters as displayed in Figure 1 was utilized for the K_x predictions. Figure 1 displays an MLP network with four input variables of (B, H, U, U^*), one hidden layer with arbitrary neurons, and one output parameter, K_x . The input-output formulation of neurons in the hidden layer is calculated by the action of the nonlinear transfer

function as [34]:

$$f(Y_{\text{net}}) = f\left(\sum_{l=1}^N w_{l,i} X_{i,j} + \alpha_l\right) \quad (3)$$

In which, $X_{i,j}$ is the input vector, y_{net} is the output of the network, $w_{i,j}$ is the connection weights from the input node to hidden nodes, a_i are the bias values of nodes, and N is equal to the number of input parameters. $f()$ is the nonlinear activation function which in this study is the 'tansig' function:

$$y_j = \frac{2}{(1 + \exp(-2x_j))} - 1 \quad (4)$$

In which, X_j is the input, and Y_j is the output of the activation function. The $w_{i,j}$, and b_i are the unknown constants that should be determined by the training scheme and in the current study are decision variables in the optimization space. The output of the model is K_x and calculated as:

$$K_x = f_0 \left[\sum_j w_{m,l} f \left(\sum_i w_{l,i} X_l + b_i \right) + b_m \right] \quad (5)$$

Here, $w_{m,l}$ is the connection weights of the hidden node to the output node, and b_m is the bias for output node. Therefore, we have used one hidden layer ANN hybridized with PSO, CSO learning schemes, and the best explicit equation is derived finally. For this purpose, the weights and biases are used as the decision parameters to minimize the mean squared error (MSE) as the goal function:

$$MSE = \frac{1}{N} \sum_{i=1}^N (K_{x_o} - K_{x_p})^2 \quad (6)$$

where K_{x_o} and K_{x_p} are observed and predicted values of the K_x and N is the number of training sets.

B. CAT SWARM OPTIMIZATION ALGORITHM

One of the nature-inspired meta-heuristic optimization algorithms is Cat Swarm Optimization (CSO), which was proposed in 2007 by Guo *et al.* [50] and improved in 2015 by Bozorg-Haddad [51]. The CSO is inspired by the cats' behavior. For this purpose, two modes, including seeking mode and tracing mode are proposed. Seeking and tracing modes are related to resting the cats and chasing the prey, respectively. The mixture of these two modes will result in a global solution. Based on Chu and Tsai (2007) and Bozorg-Haddad, (2017), the hybridized framework is provided in Figure 2, in which five steps are considered for CSO algorithm as follows:

- (1) Initialization: in this step, cats are generated and distributed randomly into M -dimensional solution space ($X_{i,d}$), and a random velocity assigns to each cat ($v_{i,d}$).
- (2) Based on the mixture ratio (MR), the population of the cats divides into two subgroups (seeking and tracing modes).
- (3) Evaluation: evaluate the fitness function of each cat. If the current position of the cat leads to a better fitness

function, then save the position of the cat as the best solution (X_{best}).

- (4) Movement: moving the cats based on the seeking and tracing modes according to the decision made up in step 1 [52].
- (5) If the stopping criteria are satisfied, the algorithm will be terminated. Otherwise, steps 2 to 5 will be repeated.

C. PARTICLE SWARM OPTIMIZATION ALGORITHM

PSO is a meta-heuristic method, which was inspired by the swarming habits of animals such as birds or fish. It combines two methodologies: artificial life and evolutionary computation [53]. Based on this algorithm, a group of particles is distributed in the N -dimensional space that N shows the number of variables, which must be optimized [54]. Each particle in the search space maintains the position, velocity, and individual best position.

Suppose an N -dimensional search space. The PSO algorithm starts with a position of i -th particles of the swarms $P_i = (p_{i1}, \dots, p_{iN})$ and the velocity $V_i = (v_{i1}, \dots, v_{iN})$ which moves them to a new location $X_i = (x_{i1}, \dots, x_{iN})$ [55]. In each iteration, the particles are updated by the two best values, the personal best position (Pbest) and the best value among all personal bests (Gbest). Each particle's velocity is updated based on the following equation:

$$v_i(t+1) = \omega v_i(t) + c_1 r_1 [\hat{x}_i(t) - x_i(t)] + c_2 r_2 [g(t) - x_i(t)] \quad (7)$$

where ω is the inertial coefficient, c_1 and c_2 are the acceleration coefficients in the range of [0,2], r_1 and r_2 are random values ($0 < r_1, r_2 < 1$) which regenerated in every update with uniform distribution, $v_i(t)$ and $x_i(t)$ are the particle's velocity and position at time t , respectively and $\hat{x}_i(t)$ is the particle's individual best solution at time t . Also, the location of particle i can be calculated according to the following equation:

$$x_i(t+1) = x_i(t) + v_i(t+1) \quad (8)$$

This algorithm is repeated until the stopping criteria satisfy. The flowchart of the PSO algorithm and its calculation procedure hybridized with the ANN in the K_x estimation is presented in Figure 3.

D. HYBRIDIZATION FRAMEWORK AND EVALUATION CRITERIA

As stated, we hybridized the PSO and CSO algorithms to train the ANN model and find the unknown values of weights and biases in equations 3, 4, and 5 by minimizing the objective function in equation 6. The model development framework and the flowchart of the study presented in Figures 2 and 3. As these figures show at first, we used train sets to find the best values of weights and biases in ANN by the minimization of the objective function by using the PSO and CSO algorithms. In iterative ANN-PSO and ANN-CSO algorithms, the optimized values of ANN weights and biases are derived

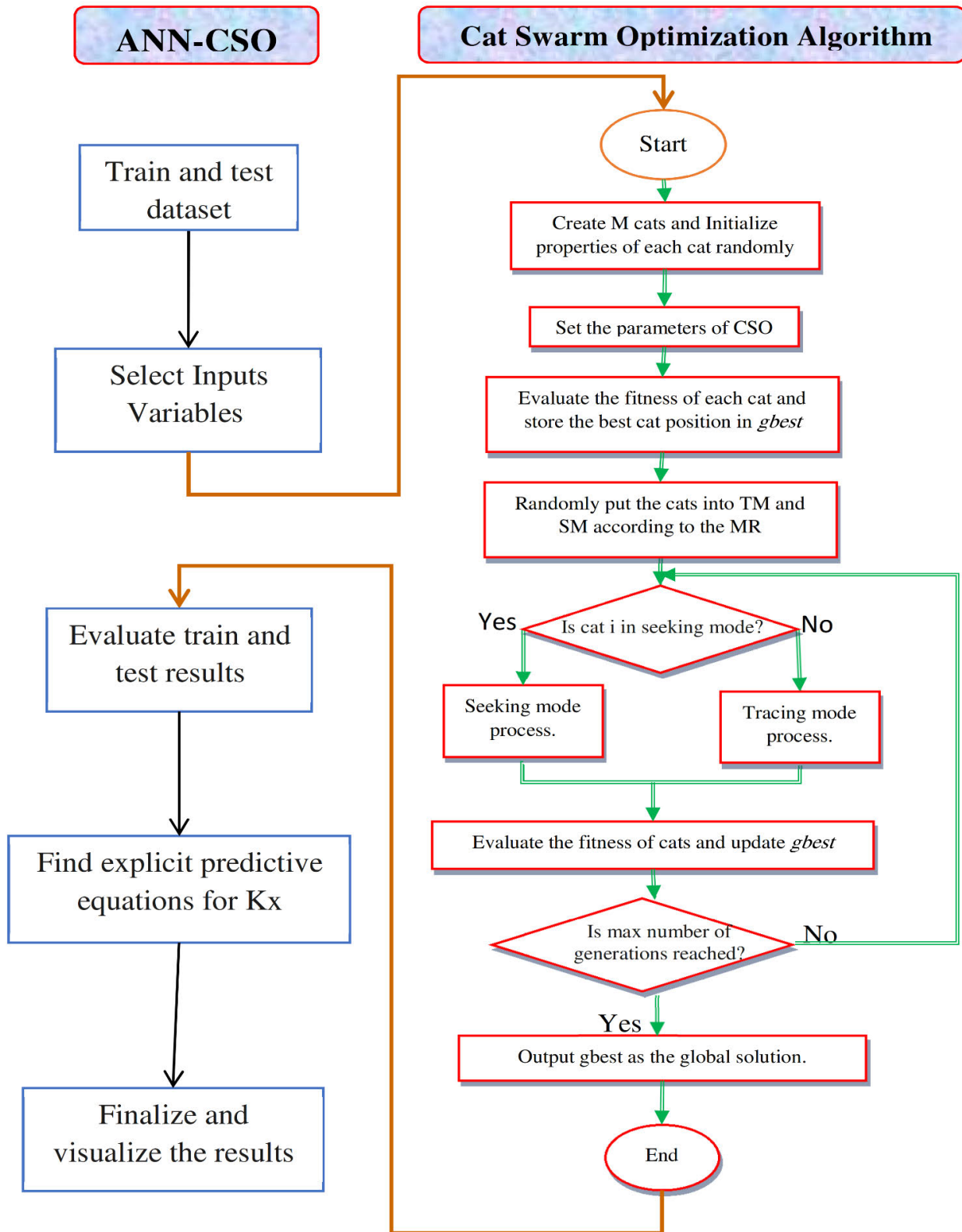


FIGURE 2. Flowchart of ANN-CSO model for estimating K_x .

and associated with the final network of models compared to the classical ANN structure to simulate the test data set. Moreover, the optimized weights and biases are implemented

in the model structure to derive optimal explicit equations for the K_x . In order to evaluate the improvements of developed hybrid, the same train and test sets and the corresponding

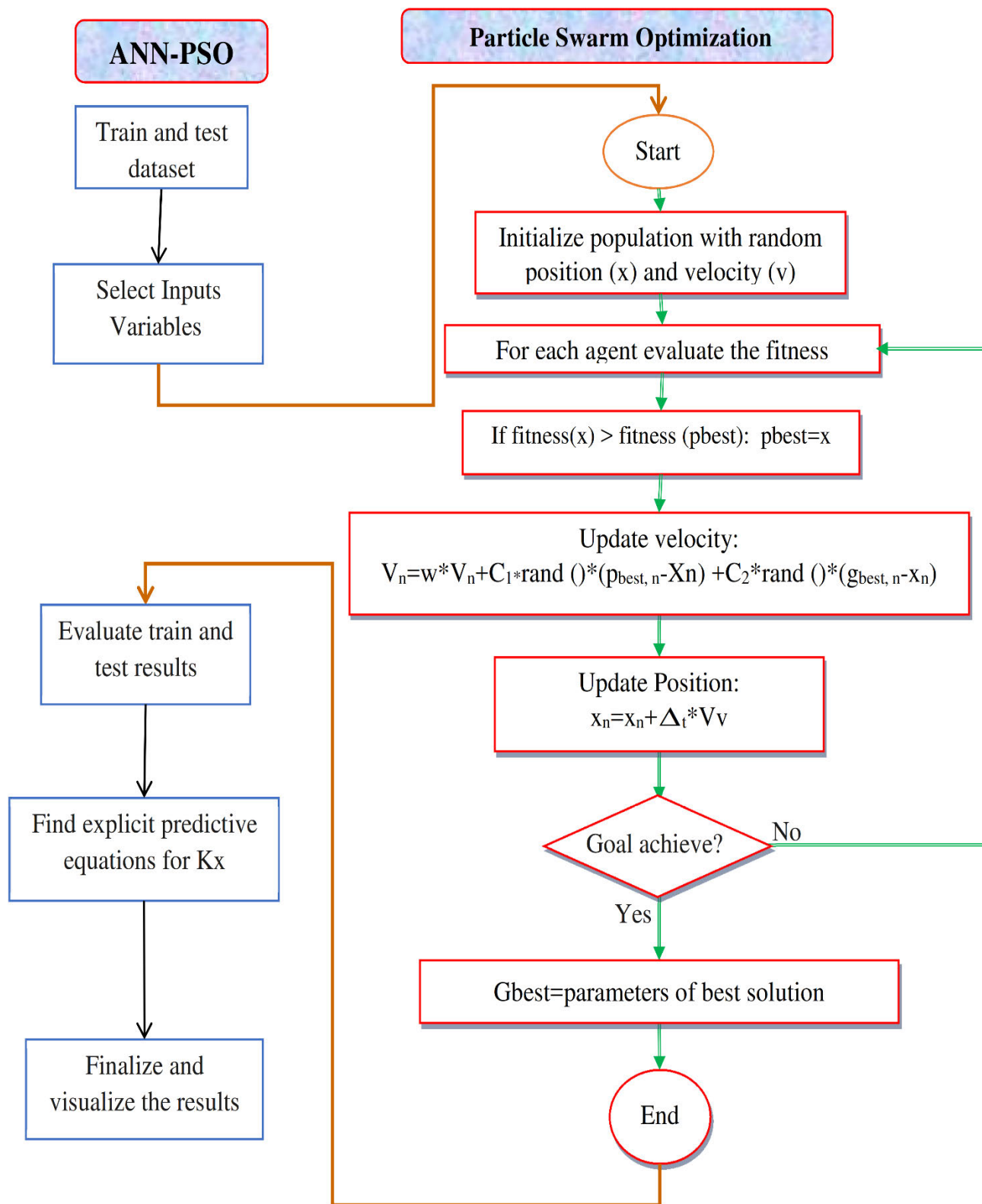


FIGURE 3. Flowchart of ANN-PSO model for estimating Kx.

input parameter combination with the study in 2005 by Tayfur and Singh [3] are used. The primary input vector includes B, H, U, and U* parameters. Additional seven combinations

of inputs used as a sensitivity analysis in the model evaluations and are presented in Table 1. Overall, 36 different models (three training schemes: PSO, CSO, classical

TABLE 1. Different input combinations used for hybrid ANN models.

Model	Input Parameters	Output
M1	U, H, B	K _x
M2	Q	K _x
M3	U	K _x
M4	U, b	K _x
M5	U, b, a	K _x
M6	U/U*	K _x
M7	U/U*, b, a	K _x
Basic	B, H, U, U*	K _x

back-propagation with eight input combinations; eight models of Tayfur and Singh [3]; four empirical equations) are used. The results are compared with the results of eight models in Tayfur and Singh [3] and four empirical equations of the K_x as provided in Table 1. Researchers have developed several empirical equations for prediction of K_x based on classical regression methods that are presented in Table 1. these equations calculates the K_x values using parameters based on the average conditions of river flow including average depth, average velocity, shear velocity and width of river. In the current study the presented empirical equations in Table 1 are compared with the results of explicit optimized equations based on ANN-CSO, ANN-PSO. The results of all 36 models are evaluated by the use of the RMSE, mean absolute error (MAE), Nash-Sutcliffe Efficiency (NSE), coefficient of determination (R²), index of agreement (d), persistence index (PI), confidence index (CI), and relative absolute error (RAE).The formulation and detailed description of these statistical indices are presented elsewhere [37], [56]–[60]. Furthermore, scatter plots, trend comparisons, box plot of errors, Taylor diagrams and error frequency distributions were used for graphical verification of model results. The accuracy of predictive models in training and testing steps is evaluated. The preference is to the R², NSE followed by RMSE and RAE for validation of the models results over unseen data in the testing stage.

$$\frac{K}{HU^*} = \frac{0.15}{8\varepsilon_t} \left(\frac{U}{U^*}\right)^2 \left(\frac{B}{H}\right)^{1.67}$$

Deng et al. (2001) [25]

$$\varepsilon_t = 0.145 + \frac{\left(\frac{U}{U^*}\right) \left(\frac{B}{H}\right)^{1.38}}{3520} \tag{9}$$

Fischer (1975) [6]

$$\frac{K}{HU^*} = .011 \left(\frac{U}{U^*}\right)^2 \left(\frac{B}{H}\right)^2 \tag{10}$$

Seo and Cheong (1998)[17]

$$\frac{K}{HU^*} = 5.92 \left(\frac{U}{U^*}\right)^{1.43} \left(\frac{B}{H}\right)^{.62} \tag{11}$$

$$\frac{K}{HU^*} = 10.612 \left(\frac{U}{U^*}\right)^2 \frac{B}{H} > 50$$

Kashefipour and Falconer (2002) [14]

$$\frac{K}{HU^*} = \left[7.428 + 1.775 \left(\frac{B}{H}\right)^{.62} \left(\frac{U}{U^*}\right)^{.572} \right] \times \left(\frac{U}{U^*}\right)^2 \frac{B}{H} < 50 \tag{12}$$

E. FIELD DATABASE OF K_x

As stated previously, geometric and hydrodynamic parameters, including H, U*, U, and B affect the longitudinal dispersion. In this study, the data provided in 2005 by Tayfur and Singh [3] are used to predict the longitudinal dispersion coefficient due to their general acceptability in different studies over the K_x predictions. These field data have measured K_x on different rivers over 29 rivers in the United States. The database obtained from Tayfur and Singh [3], and the train and test sets are the same as used by them. The plots of distribution and variations of K_x in the train and test steps versus the other input parameters are shown in Figure 4. The statistical characteristics of the data in the train, test and all of the data are presented in Table 2. It is apparent that all parameters have nearly equal distribution over train and test subsets and this database covers an extensive range of K_x ranged from 1.9 to 892m²/s in all, and 1.9 to 837 m²/s in the train set and 2.9 to 892 m²/s in the test set. Furthermore, the standard deviation of the K_x values of the training subset is higher than the test subset and it indicates that using this dataset, the developed models will provide reliable predictions for unseen data and this will eliminate the overfitting of models in the training sets.

III. RESULTS AND DISCUSSIONS

A. ALGORITHMS COMPARISONS: ANN-PSO, ANN-CSO AND ANN

To evaluate the efficiency of developed algorithms, we compare the CSO, PSO algorithm results with the standalone ANN training algorithm and the best model results are compared with the results of Tayfur and Singh [3]. As presented in Table 1, we used the main model with input vector of B, H, U, U* and in this section, the comparison of algorithms is based on this structure. The results of ANN, ANN-PSO, ANN-CSO and the ANN of Tayfur and Singh [3] in the base model are listed in Table 3 in the training stage. It can be detected that the developed ANN-PSO model in the training stage has the highest R², NSE and PI values equal to 0.96, 0.96 and 0.94, respectively with the lowest values of RMSE, MAE and RAE equal to 29.12, 21.74 and 0.24, respectively. These statistical indices confirm the superiority of the PSO

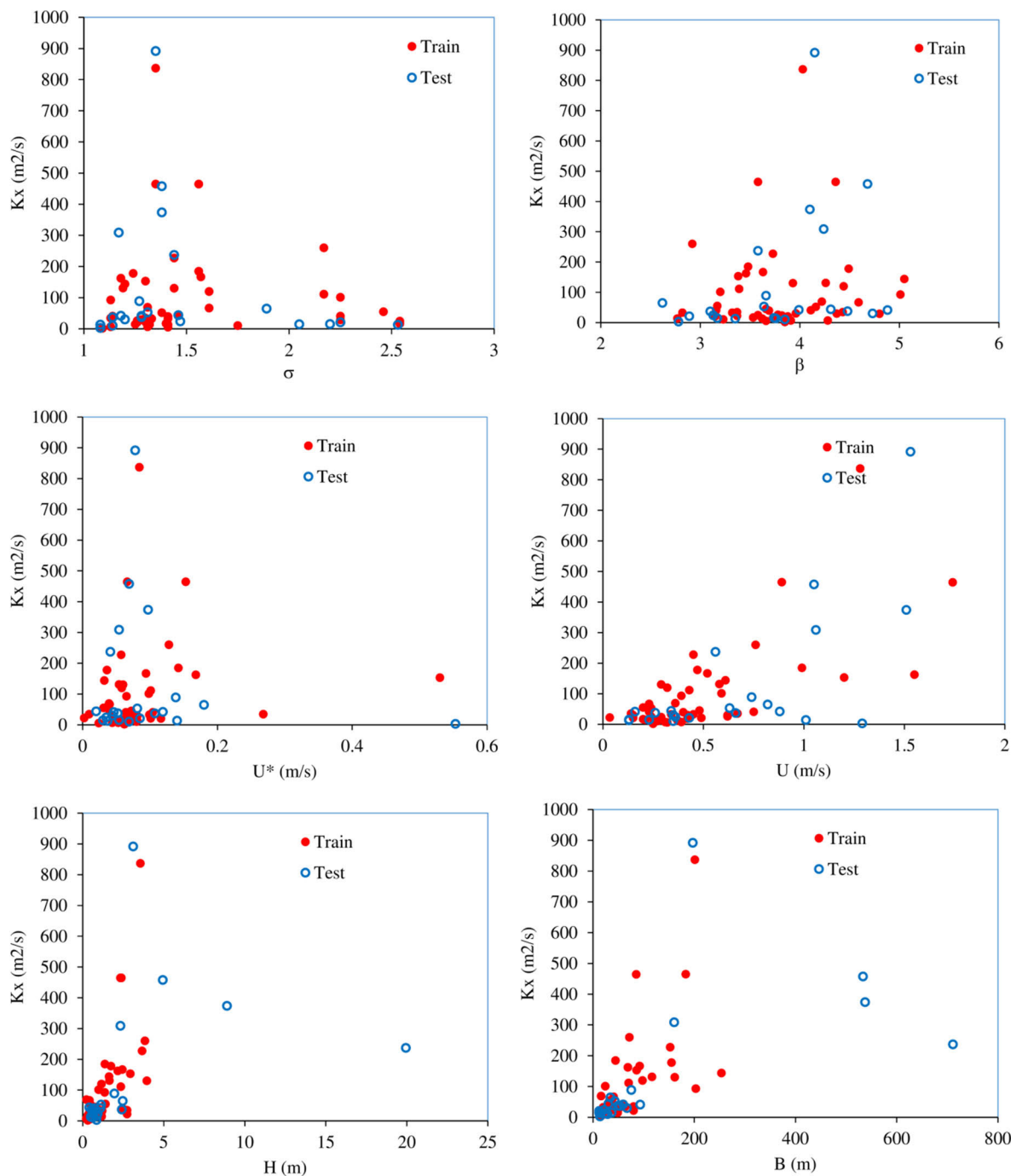


FIGURE 4. The plot of the distribution of field K_x data in the train and test sets according to the different input parameters.

algorithm in the training stage in terms of agreement, persistence, confidence and accuracy. Hence, in the training stage of the basic model, it ranks the first among all other training methods. In addition, results in ANN, ANN-CSO and ANN-Tayfur and Singh [3] are so close to each other. It confirms that hybridizing with PSO would be satisfying for improving the accuracy of the data-driven model.

To have a clear sight of performances of the developed models, in Fig. 5a the predicted versus observed values of K_x in the training stage are plotted. It is clear that the ANN-PSO model acts significantly better than the previous standalone ANN models, and the ANN-CSO also has better performance than the standalone ANN models, especially over peak values of the K_x . These results support the idea of applying

TABLE 2. Statistical criteria for the train, test and over all of the datasets.

Parameter	Mean	Mode	SD	Min.	First Quart	Median	Third Quart	Max.	Skew.	Kurt.	
Total data	B (m)	82.96	13.00	122.50	11.90	20.00	42.20	83.98	711.20	3.42	15.55
	H (m)	1.71	0.81	2.60	0.22	0.52	0.91	2.33	19.94	5.27	35.92
	U (m/s)	0.54	0.23	0.39	0.03	0.28	0.42	0.67	1.74	1.34	4.18
	u*(m/s)	0.09	0.07	0.09	0.00	0.05	0.07	0.10	0.55	3.93	20.20
	B/H	51.68	23.90	31.72	13.80	29.25	41.80	67.23	156.50	1.43	4.77
	U/U*	7.62	2.50	4.56	1.29	4.56	6.32	9.23	19.63	1.04	3.26
	b	3.79	3.58	0.57	2.62	3.37	3.74	4.21	5.05	0.18	2.51
	s	1.51	1.30	0.42	1.08	1.26	1.35	1.57	2.54	1.34	3.48
	K_x(m²/s)	107.71	13.90	170.25	1.90	20.73	39.50	127.83	892.00	2.95	12.40
Train data	B (m)	62.93	13.00	58.83	12.80	19.28	42.00	81.33	253.60	1.54	4.62
	H (m)	1.34	0.81	1.06	0.22	0.48	0.91	2.20	3.96	1.02	2.95
	U (m/s)	0.49	0.29	0.35	0.03	0.27	0.39	0.60	1.74	1.84	6.34
	u*(m/s)	0.08	0.07	0.08	0.00	0.05	0.07	0.10	0.53	4.10	23.02
	B/H	51.36	29.20	31.31	16.00	29.70	41.60	65.08	156.50	1.68	5.80
	U/U*	7.13	2.50	4.02	1.29	4.48	6.09	9.05	19.06	1.00	3.41
	b	3.79	3.37	0.53	2.77	3.39	3.73	4.18	5.05	0.35	2.75
	s	1.53	1.30	0.42	1.09	1.28	1.35	1.58	2.54	1.37	3.52
	K_x(m²/s)	98.43	13.90	148.27	1.90	20.78	39.50	130.70	837.00	3.21	14.77
Test data	B (m)	127.59	11.90	197.71	11.90	25.00	45.85	93.00	711.20	2.02	5.64
	H (m)	2.55	0.40	4.35	0.40	0.59	0.90	2.41	19.94	3.23	13.03
	U (m/s)	0.66	0.13	0.44	0.13	0.34	0.60	1.01	1.53	0.60	2.27
	u*(m/s)	0.10	0.05	0.11	0.02	0.04	0.07	0.11	0.55	3.45	14.90
	B/H	52.40	13.80	33.34	13.80	23.90	42.70	69.10	131.00	0.92	2.90
	U/U*	8.72	2.33	5.52	2.33	5.00	7.30	13.66	19.63	0.81	2.33
	b	3.77	2.62	0.65	2.62	3.17	3.75	4.24	4.88	-0.03	2.06
	s	1.48	1.08	0.42	1.08	1.18	1.33	1.47	2.53	1.27	3.33
	K_x(m²/s)	128.40	2.90	213.82	2.90	15.50	39.60	88.90	892.00	2.42	8.55

optimization algorithms for the longitudinal dispersion equation finding. It is apparent that the results predicted by the ANN-PSO model are superior to the others. The scatter plot of the training stage is also presented in Fig. 5b that reveals the

superiority of ANN-PSO to the other methods. As described in the previous sections, the main strategy for improving the accuracy of the ANN models is using the benefits of hybrid training methods. Among the different strategies that are

TABLE 3. Comparison of models results in the train and test stages.

	Train				Test			
	Tayfour and Singh (2005)	PSO	CSO	ANN	Tayfour and Singh (2005)	PSO	CSO	ANN
R²	0.89	0.96	0.83	0.85	0.70	0.94	0.81	0.67
RMSE	49.75	29.12	63.43	62.73	184.04	81.47	137.39	224.57
MAE	33.19	21.74	44.67	42.73	85.90	51.72	73.56	123.98
PI	0.84	0.94	0.73	0.73	0.34	0.87	0.75	0.54
RAE	0.36	0.24	0.48	0.46	0.58	0.35	0.50	0.84
d	0.97	0.99	0.95	0.95	0.86	0.97	0.92	0.82
NSE	0.89	0.96	0.81	0.82	0.22	0.85	0.57	-0.16
CL	0.86	0.95	0.77	0.78	0.19	0.82	0.52	-0.13

used, the standalone ANN method shows the weakest results (Fig. 5) and indicates that hybrid models play an effective role.

A three-aspect comparison based on correlation coefficient, standard deviation and centered root mean square difference (RMSD) for each of the models when compared with each of the observed the Kx data sets (shows with the actual label in the horizontal axis), is shown in Figure 6a as Taylor diagram. Taylor diagram is a single diagram that summarizes multiple indices of assessment results, the RMSE, correlation coefficient, and standard deviation. In Taylor diagrams, the performance of models is highlighted by comparing the observed and estimated values by visualizing a series of points on a polar diagram. The reference point is the observed values located by standard deviation that here is 150 and 205 m²/s in the train and test sets, respectively. The azimuth angle of the plot displays the correlation coefficient of observed and estimated Kx values, and the radial distance from the reference point shows the ratio of normalized standard deviation of the simulation from the measured values. Each point in this plot displays the accuracy of each model, and models with more accurate estimations are closer to the reference point. The values of the RMSD are shown using the observed Kx data set as a reference of actual values. The lowest value for RMSD in the training set is 30 for the ANN-PSO with the highest value of correlation coefficient, 0.98 in Figure 6a. In addition, the empirical cumulative probability of absolute error of models in the training stage is presented in Figure 6b. Based on the results in Figure 6b, for absolute error of 5 m²/s, the highest probability is 0.9 in ANN-PSO model and shows that with the probability of 90%, the absolute error of ANN-PSO is lower than 50 m²/s, while for ANN-CSO, it is equal to 140, in Tayfur and Singh is equal to 115 and in ANN is equal to 150 m²/s. As this figure shows,

the ANN-PSO estimated the Kx values with smaller error, and the probability of the estimated Kx via the ANN-PSO with a given absolute error in the train stage is higher than the other models. These results show the accurate performance of ANN-PSO in the training stage and the other models, including ANN, and ANN-CSO have similar accuracy in the training stage. However, the efficiency of models in the testing stage as an application of the intelligence model is crucial and in the next section is discussed.

B. ANALYSIS OF THE RESULTS

The results of developed models in the test stage of the main model with four inputs of B, H, U, U* are presented in Table 3. According to the presented results in this table, the hybridized models of ANN-PSO and ANN-CSO have the best performances than the ANN and previous ANN by Tayfur and Singh [3]. This table shows that the CSO and PSO training algorithms provide more reliable and accurate predictions for Kx than the standalone models. For example, the R² values of ANN-PSO and ANN-CSO models are 0.94 and 0.81, respectively, while the R² of the ANN model is less than 0.7. The higher values of R² in the hybrid models in the testing stage demonstrates a relatively high correlation between the observed and estimated values of Kx. Table 3 also confirms that the hybridizing schemes of training improve the performance of the standalone ANN model in the test stage about 34% and 18 % in terms of R² for PSO and CSO, respectively. The hybridization of the ANN model also reduces the RMSE by 55% for PSO and 26% for CSO. In Figure 7, the observed and predicted values of Kx in different models at the test stage are presented. The ANN-PSO model provides estimations closer to the observed values for both large and small values and its predictions in

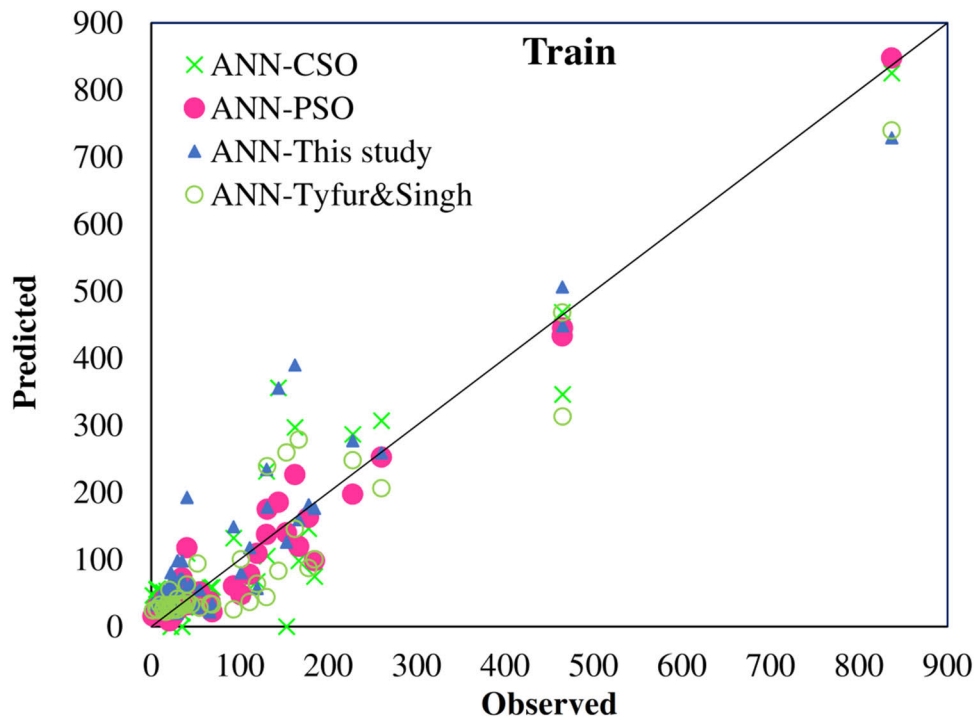
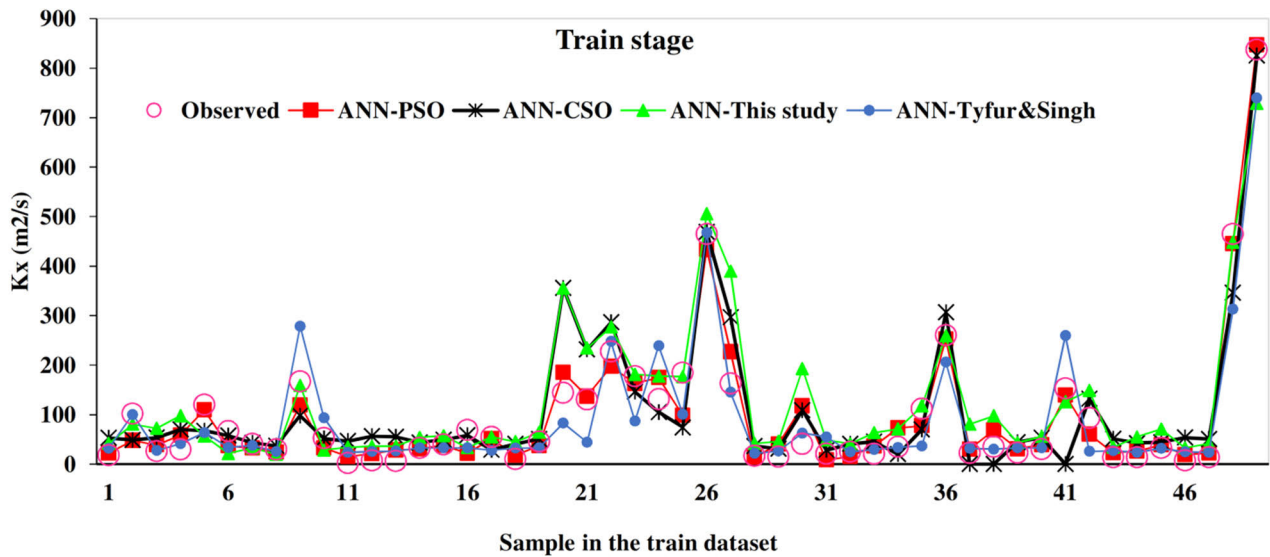


FIGURE 5. Comparison of models results in the training stage, a) observed versus predictions b) scatter plot of models.

peak values are useful. Moreover, the ANN-CSO model has better predictions in the test step than the stand-alone ANN models.

In Figure 8, the Taylor diagram and cumulative probability of prediction errors in the test step are presented. As Taylor diagram in Figure 8a shows, the best model and closer to the reference point is ANN-PSO with standard deviation of 235 m^2/s close to the 200 m^2/s in observed values. This parameter in ANN-CSO is 275 m^2/s , in ANN is 325 m^2/s and

in ANN-Tayfur and Singh (2005) is 300 m^2/s . The RMSD values in the train step of ANN-PSO is the lowest and equal to 60, in ANN-CSO is 120, in Tayfur and Singh (2005) is 170 and in ANN is 190 which confirms the superiority and great improvements in the ANN-PSO and ANN-CSO models than the others. Also, Figure 8b shows that with probability of 90%, the absolute error in ANN-PSO and ANN-CSO are nearly less than 100 m^2/s , while these values for ANN and Tayfur and Singh (2005) are 300 and 350 m^2/s , respectively.

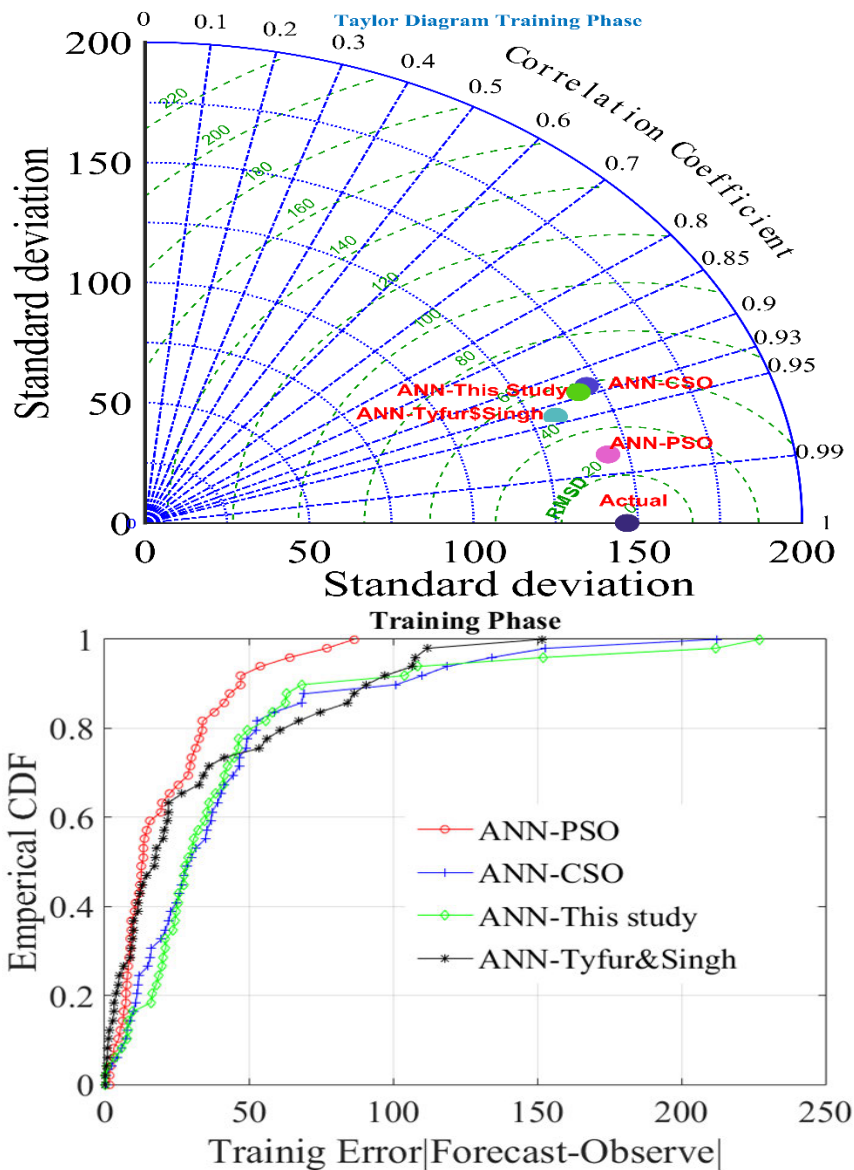


FIGURE 6. a) Taylor diagrams the correlation, RMSD, standard deviation of models versus actual values in train stage, b) probability of absolute errors.

Again, these values confirm the higher reduction of error predictions in test stage of ANN-PSO and ANN-CSO in comparison versus standalone ANN models. The result of models in the test stage in Figures 7 and 8 and Table 4 show that using PSO and CSO algorithms to train ANN strongly improves the model accuracy, persistence, reliability and performance. In the test stage, both PSO and CSO optimization algorithms are superior to the classical algorithms in the training ANN. These findings indicate that the proposed hybrid models are able to provide an accurate estimation of K_x values with a great performance over various ranges of K_x values in the current study. The results in Figure 8 evidently confirm the improvements in K_x predictions by ANN-CSO and ANN-PSO versus the previous models of ANN. It is proven

that the developed hybrid models can be used effectively to predict the K_x coefficient in natural river flows. Higher values of R^2 , NSE and d are associated with small values of RMSE, MAE and RAE in the testing stage of the hybrid models.

C. SENSITIVITY ANALYSIS TO THE INPUT FEATURES

In order to investigate the effects of different input combinations and evaluate the sensitivity of the hybrid model results with input parameters, the sensitivity analysis of the developed ANN-based models were carried out by estimating the observed K_x values in seven cases (Table 1). These seven M1 to M7 models are trained and tested using the same data as those used by Tayfur and Singh (2005) and the results of them are presented here in the testing stages. These seven cases

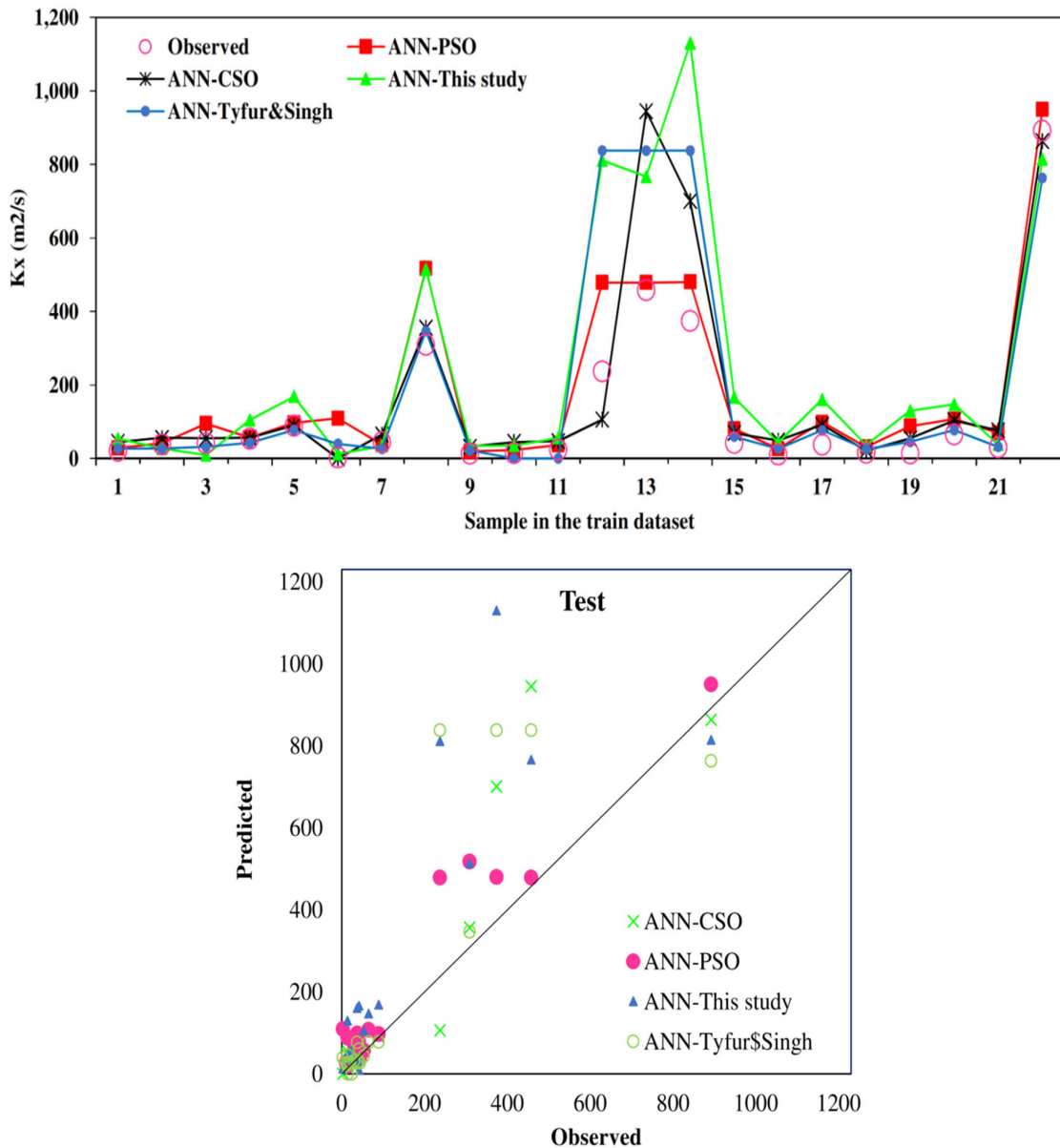


FIGURE 7. Comparison of models results in the testing stage, a) observed versus predictions b) scatter plot of models.

are based on the physically meaning of hydraulic flow and pollutant dispersion as suggested by Tayfur and Singh (2005). In the M1 model, the input parameters are only U , H , B as the main hydraulic effective parameters. As the results of models in Table 4 show, in M1 model, the best results are derived by the ANN-PSO and ANN-CSO models with R^2 values of 0.91 and 0.93 and RMSE values of 83.42 and 81.42, respectively that confirm 32% and 35% improvements in R^2 and 57% and 58% reduction in RMSE values, respectively than the classical ANN model. In the M2 model, the input parameter is only flow discharge (Q), indeed it is a product of three parameters of U , H , B in case M1. In the M2 model, the best results are those predicted by ANN-PSO and ANN-CSO with 32% and 8% improvements in R^2 values

and 75% and 15% reductions in RMSE values, respectively compared to the classical ANN model.

In M3, the input vector is only U . The velocity and its gradients are crucial in the magnitude and strength of longitudinal dispersion in river flows [5]. As the results in this case show, the accuracy of models reduced, and the R^2 values are near 0.4, which show that the geometry parameters are also needed for a suitable prediction. The M4 uses the velocity U and the shape parameter (b) as input variables to predict K_x . The results of the M4 models show that using the shape parameter improves the model accuracy and in this case the R^2 values increased from 0.4 in the M3 model to 0.7 in M4 model. Also, PSO and CSO based models were superior to the others. In the M5, the input parameters are velocity U along with the

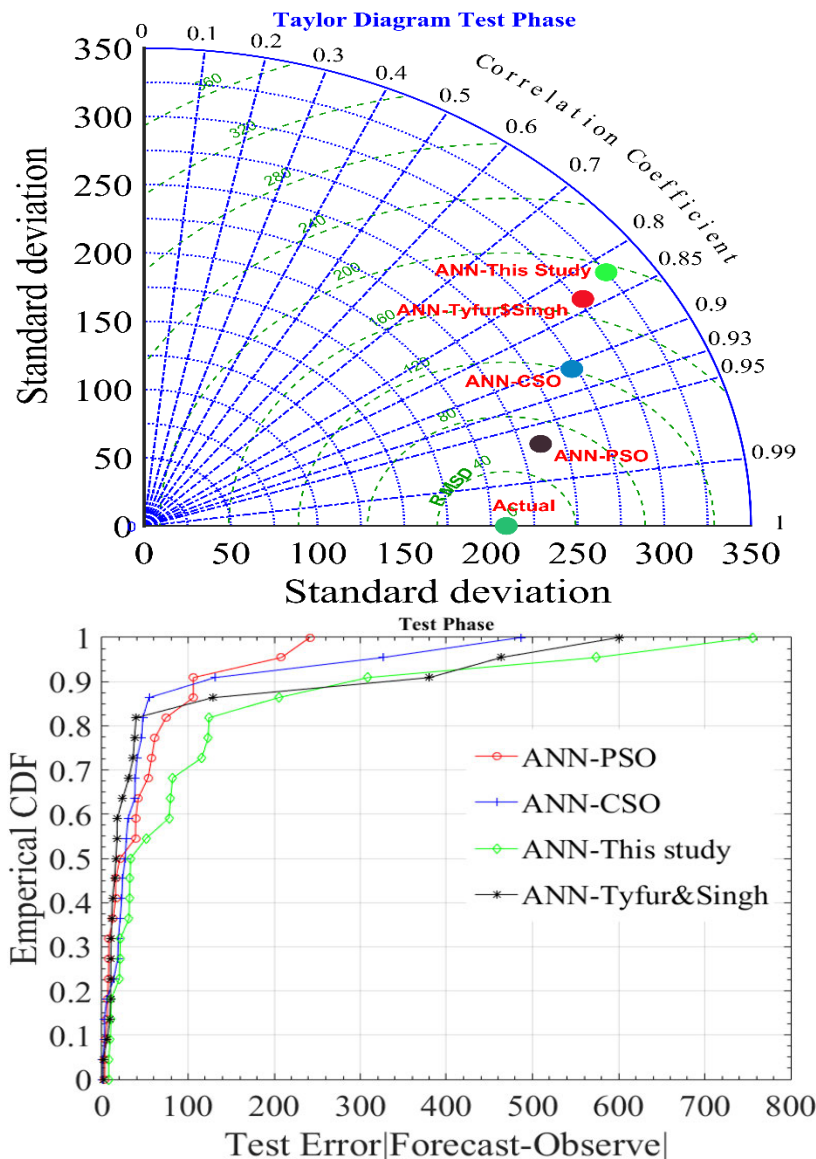


FIGURE 8. a) Taylor diagrams the correlation, RMSD, standard deviation of models versus actual values in test stage, b) probability of absolute errors.

shape factor b and the sinuosity s . This input combination resulted in the reduction of RMSE from 119.17 to 99.35 for the ANN-PSO model as the most accurate model in this class. As M4 and M5 show, the addition of shape factor and sinuosity to the input vectors increased the accuracy of model than the M3 model with U input. However, in comparison with the case M2, using U and B is more effective than using b and s . In the M6 model, the only input parameter is the relative shear velocity (U/U^*) that is usually used in empirical equations of K_x , such as equation 9-12. In the M6 model, the R^2 values are in the range of 0.52-0.61 and relatively smaller than the values in M1, M2, M4 and M5 models. Finally, the case M7 uses U/U^* with b and s as input values and shows somewhat improvements compared to the M6 model but less accuracy than the M1, M2, M4 and M5 cases. A comparison

of different input combinations shows that appropriate selection of the input parameters for prediction of K_x plays a crucial role in model accuracy.

Figure 9 demonstrates the results of the different models in the sensitivity analysis of input parameters in terms of the Taylor diagram. As it can be inferred, the hybridizing of the ANN with the PSO and CSO algorithms significantly outperforms the classical ANN results. Overall comparison of the sensitivity analysis in Figure 9 reveals that the ANN-PSO2 model that uses Q as input, ANN-CSO1 and ANN-PSO1 models that use U , H , B as input are more accurate and superior than the others. The reason for differences of the model performances in Figure 9 is related to the training method and input vectors of each model that could be disclosed with a look to Table 1. Therefore, it is concluded

TABLE 4. The results of different models in the sensitivity analysis.

		R²	RMSE	MAE	PI	RAE	d	NSE	CL
M1	Tyfur/ Singh(2005)	0.69	192.89	93.24	0.34	0.59	0.86	0.20	0.17
	PSO	0.91	83.42	50.82	0.88	0.32	0.97	0.85	0.82
	CSO	0.93	81.42	47.50	0.91	0.30	0.97	0.86	0.83
	ANN	0.62	145.09	81.94	0.68	0.52	0.88	0.55	0.48
M2	Tyfur / Singh(2005)	0.41	169.56	111.65	0.49	0.71	0.76	0.38	0.29
	PSO	0.41	169.14	109.90	0.50	0.70	0.76	0.39	0.29
	CSO	0.45	162.11	108.45	-0.03	0.69	0.76	0.44	0.33
	ANN	0.42	167.26	110.89	-0.01	0.70	0.76	0.40	0.30
M3	Tyfur / Singh(2005)	0.72	116.34	71.24	0.76	0.45	0.90	0.71	0.64
	PSO	0.79	99.35	61.23	0.83	0.39	0.93	0.79	0.74
	CSO	0.74	115.16	85.94	0.68	0.55	0.92	0.72	0.66
	ANN	0.70	122.56	86.51	0.64	0.55	0.91	0.68	0.62
M4	Tyfur / Singh(2005)	0.73	190.63	94.65	0.36	0.60	0.86	0.22	0.19
	PSO	0.96	47.15	32.10	0.96	0.20	0.99	0.95	0.94
	CSO	0.79	161.09	80.23	0.73	0.51	0.90	0.44	0.40
	ANN	0.60	199.03	93.37	0.58	0.59	0.84	0.15	0.13
M5	Tyfur / Singh(2005)	0.47	160.61	98.24	0.54	0.62	0.81	0.45	0.36
	PSO	0.73	119.17	88.10	0.75	0.56	0.91	0.70	0.63
	CSO	0.74	115.82	81.96	0.61	0.52	0.91	0.71	0.65
	ANN	0.71	119.02	77.76	0.47	0.49	0.90	0.70	0.62
M6	Tyfur / Singh(2005)	0.54	158.78	86.91	0.56	0.55	0.72	0.46	0.33
	PSO	0.61	150.41	84.32	0.60	0.54	0.76	0.52	0.39
	CSO	0.58	160.23	86.88	-0.17	0.55	0.70	0.45	0.32
	ANN	0.52	179.71	106.49	-0.34	0.68	0.63	0.31	0.19
M7	Tyfur / Singh(2005)	0.60	138.66	81.49	0.66	0.52	0.84	0.59	0.49
	PSO	0.61	150.41	84.32	0.60	0.54	0.76	0.52	0.39
	CSO	0.61	136.80	71.95	0.46	0.46	0.85	0.60	0.51
	ANN	0.55	152.44	104.24	0.60	0.66	0.86	0.50	0.43

TABLE 5. Comparison of statistical indicators in hybrid versus empirical equations.

Statistical criteria	Kashefipour and Falconer (2002)	Deng et al. (2001)	Seo and Cheong(1998)	Fischer (1975)	PSO-Eq	CSO-Eq
R ²	0.42	0.43	0.45	0.37	0.94	0.81
RMSE	282.98	327.40	436.68	1708.37	81.47	137.39
MAE	88.29	94.58	134.65	529.70	51.72	73.56
PI	0.20	0.19	0.15	0.04	0.87	0.75
RAE	0.81	0.87	1.24	4.88	0.35	0.50
d	0.66	0.63	0.55	0.20	0.97	0.92
NSE	-1.80	-2.75	-5.67	-101.13	0.85	0.57
CL	-1.20	-1.72	-3.12	-19.92	0.82	0.52

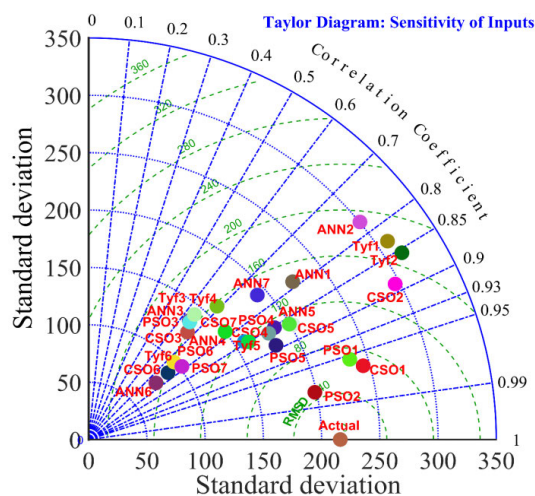


FIGURE 9. Taylor diagram for the results of all different models of sensitivity analysis in test stage.

that applying hybrid ANN-based models will be suitable if an appropriate set of inputs is used.

D. OPTIMIZED EQUATIONS

As mentioned, another aim of the current study is to derive predictive equations for Kx based on optimized ANN models. The black-box form of the traditional ANN models is very complicated and maybe less applicable in future studies for estimation of Kx. Therefore, here we have used the optimized values of weights in ANN-based structures to find an explicit equation. The equation-based form of ANN is one of the advantages of the developed hybrid models in this study, which is commonly used in pollutant transport models. As stated in previous sections, the best models in the test stage were ANN-PSO and ANN-CSO models that use four input

parameters of B, H, U and U*. Here the optimized equation of each hybrid model is presented as an explicit equation. The ANN-PSO based equation is derived as:

$$\begin{aligned}
 A_1 &= 1 + e^{-0.02B+0.39H+3.52U+11.37u*-3.72} \\
 B_1 &= 1 + e^{0.02B-0.48H+0.69U+11.37u*+2.37} \\
 C_1 &= 1 + e^{0.02B+0.87H-3.52U-2.04u*-4.48} \\
 D_1 &= 1 + e^{0.03B+1.60H+3.52U-4.49u*-11.6} \\
 K_x &= \frac{-124.74}{A_1} + \frac{374.99}{B_1} - \frac{517.15}{C_1} - \frac{636.76}{D_1} + 227.59
 \end{aligned}
 \tag{13}$$

It should be noted that the results of this equation are equal to the results of the developed ANN-PSO model that is presented in Figures 5 to 8 and Tables 3 and 4. In the same way, the explicit optimized equation for Kx based on the results of ANN-CSO model is derived as follows and is equal to the black-box structure of the ANN-CSO model:

$$\begin{aligned}
 A_1 &= 1 + e^{0.04B-0.62H-2.71U+23.26u*-9.21} \\
 B_1 &= 1 + e^{-0.023B+1.31H+0.54U+10.18u*+1.91} \\
 C_1 &= 1 + e^{0.021B+0.11H+2.04U-3.60u*-7.25} \\
 D_1 &= 1 + e^{0.01B+1.07H+2.14U+0.335u*-7.20} \\
 E_1 &= 1 + e^{-0.01B-0.24H+7.94U+1.49u*+2.33} \\
 K_x &= \frac{471.22}{A_1} + \frac{315.96}{B_1} - \frac{306.77}{C_1} \\
 &\quad - \frac{818.23}{D_1} - \frac{583.71}{E_1} + 688.54
 \end{aligned}
 \tag{14}$$

It should be noted that the developed explicit equations for Kx, based on the hybrid ANN models presented above are valid only for the ranges of data that are given in Table 2. The accuracy and performance of two newly developed equations are verified against the empirical equations from previous studies. In Table 5, the results of equations 13 and 14

are compared with the results of equations 9-12. As the results in this table shows, the best accurate equation is equation 13 and, after that, the ANN-CSO equation. The statistical indices show that the superiority of developed equations (13, 14) is confirmed and the previous equations have low accuracy in this regard and one can easily conclude that these equations (9-12) do not give acceptable estimations of K_x . The optimized equations outperformed in terms of accuracy (R^2 , RMSE, NSE), persistence index (PI), confidence index (CI), remarkably. Consequently, the ANN-PSO, ANN-CSO equations derived in the current study have noticeable improvements in terms of accuracy and correlation than the previous ones.

The previous studies on the longitudinal dispersion declared that black-box methods such as ANFIS, GEP, SVM and ANN models are more accurate and superior than the empirical equations [11]–[13], [20]. The black-box methods because of their capability in inferring the nonlinear problems, outperforms than the regression-based models and the results of the current study show that by employing meta-heuristic optimization algorithms in ANN training, the equations accuracy improved significantly and expected to have higher accuracy than the previous studies.

IV. SUMMARY AND CONCLUSION

In the current study, two new prediction equations for one-dimensional longitudinal dispersion coefficient were developed using hybrid models of ANN-CSO and ANN-PSO. The performances of these models in different combinations of input variables are evaluated in standalone form of ANN and in combination with the meta-heuristic optimization algorithms. The developed models are trained and tested using the data sets measured on 29 streams in the United States, that were previously used by Tayfur and Singh (2005) for the ANN model. Results revealed that the performances of newly developed hybrid models are highly satisfying and persistence and they were superior to the classical ANN and empirical equations in the previous studies. The result obtained by the hybrid ANN models of PSO and CSO were close to each other, support the idea of utilizing the meta-heuristic optimizations in training ANN. The sensitivity analysis over input parameters used to determine the effects of hydraulic and geometric parameters in the estimation of K_x . The results of sensitivity analysis showed that in all of the input combinations, the ANN-PSO and ANN-CSO models were superior to the stand-alone ANN models and improve the performance of the models significantly. As a new contribution and an application of the current study, two explicit equations are derived for prediction of K_x in terms of B , H , U and U^* parameters as input variables. The new equations are compared with the previous empirical equations and found to be more accurate and persistent than the previous equations and in good agreement with observed field values of K_x .

The developed equations are robust techniques and tools than the classical studies over the black-box ANN-based models. These new equations can be used to estimate the K_x

in one-dimensional pollutant transfer models that is essential for the pollution studies in environmental river engineering practice. As the results of the developed explicit equations based on ANN-PSO, ANN-CSO models were superior to the others, it is recommended to apply this technique in other problems to derive explicit predictive equations.

REFERENCES

- [1] E. Perucca, C. Camporeale, and L. Ridolfi, "Estimation of the dispersion coefficient in rivers with riparian vegetation," *Adv. Water Resour.*, vol. 32, no. 1, pp. 78–87, Jan. 2009.
- [2] W. Huai, H. Shi, S. Song, and S. Ni, "A simplified method for estimating the longitudinal dispersion coefficient in ecological channels with vegetation," *Ecol. Indicators*, vol. 92, pp. 91–98, Sep. 2018.
- [3] G. Tayfur and V. P. Singh, "Predicting longitudinal dispersion coefficient in natural streams by artificial neural network," *J. Hydraul. Eng.*, vol. 131, no. 11, pp. 991–1000, Nov. 2005.
- [4] A. Seifi and H. Riahi-Madvar, "Improving one-dimensional pollution dispersion modeling in rivers using ANFIS and ANN-based GA optimized models," *Environ. Sci. Pollut. Res.*, vol. 26, no. 1, pp. 867–885, Jan. 2019, doi: [10.1007/s11356-018-3613-7](https://doi.org/10.1007/s11356-018-3613-7).
- [5] M. Dehghani, M. Zargar, H. Riahi-Madvar, and R. Memarzadeh, "A novel approach for longitudinal dispersion coefficient estimation via tri-variate archimedean copulas," *J. Hydrol.*, vol. 584, May 2020, Art. no. 124662, doi: [10.1016/j.jhydrol.2020.124662](https://doi.org/10.1016/j.jhydrol.2020.124662).
- [6] M. J. Alizadeh, D. Ahmadyar, and A. Afghantoloe, "Improvement on the existing equations for predicting longitudinal dispersion coefficient," *Water Resour. Manage.*, vol. 31, no. 6, pp. 1777–1794, Apr. 2017.
- [7] C. Shen, J. Niu, E. J. Anderson, and M. S. Phanikumar, "Estimating longitudinal dispersion in rivers using acoustic Doppler current profilers," *Adv. Water Resour.*, vol. 33, no. 6, pp. 615–623, Jun. 2010.
- [8] Y. Wang and W. Huai, "Estimating the longitudinal dispersion coefficient in straight natural rivers," *J. Hydraul. Eng.*, vol. 142, no. 11, Nov. 2016, Art. no. 04016048.
- [9] Y.-F. Wang, W.-X. Huai, and W.-J. Wang, "Physically sound formula for longitudinal dispersion coefficients of natural rivers," *J. Hydrol.*, vol. 544, pp. 511–523, Jan. 2017.
- [10] V. V. C. Suarez, A. N. A. Schellart, W. Brevis, and J. D. Shucksmith, "Quantifying the impact of uncertainty within the longitudinal dispersion coefficient on concentration dynamics and regulatory compliance in rivers," *Water Resour. Res.*, vol. 55, no. 5, pp. 4393–4409, May 2019.
- [11] H. Riahi-Madvar, M. Dehghani, A. Seifi, and V. P. Singh, "Pareto optimal multigene genetic programming for prediction of longitudinal dispersion coefficient," *Water Resour. Manage.*, vol. 33, no. 3, pp. 905–921, Feb. 2019, doi: [10.1007/s11269-018-2139-6](https://doi.org/10.1007/s11269-018-2139-6).
- [12] R. Memarzadeh, H. G. Zadeh, M. Dehghani, H. Riahi-Madvar, A. Seifi, and S. M. Mortazavi, "A novel equation for longitudinal dispersion coefficient prediction based on the hybrid of SSMD and whale optimization algorithm," *Sci. Total Environ.*, vol. 716, May 2020, Art. no. 137007, doi: [10.1016/j.scitotenv.2020.137007](https://doi.org/10.1016/j.scitotenv.2020.137007).
- [13] H. Riahi-Madvar, M. Dehghani, K. S. Parmar, N. Nabipour, and S. Shamshirband, "Improvements in the explicit estimation of pollutant dispersion coefficient in rivers by subset selection of maximum dissimilarity hybridized with ANFIS-firefly algorithm (FFA)," *IEEE Access*, vol. 8, pp. 60314–60337, 2020, doi: [10.1109/ACCESS.2020.2979927](https://doi.org/10.1109/ACCESS.2020.2979927).
- [14] S. M. Kashefipour and R. A. Falconer, "Longitudinal dispersion coefficients in natural channels," *Water Res.*, vol. 36, no. 6, pp. 1596–1608, Mar. 2002.
- [15] B. Gharabaghi and A. M. A. Sattar, "Empirical models for longitudinal dispersion coefficient in natural streams," *J. Hydrol.*, vol. 575, pp. 1359–1361, Aug. 2019.
- [16] L. Gu, X.-X. Zhao, L.-H. Xing, Z.-N. Jiao, Z.-L. Hua, and X.-D. Liu, "Longitudinal dispersion coefficients of pollutants in compound channels with vegetated floodplains," *J. Hydrodyn.*, vol. 31, no. 4, pp. 740–749, Aug. 2019.
- [17] I. W. Seo and T. S. Cheong, "Predicting longitudinal dispersion coefficient in natural streams," *J. Hydraul. Eng.*, vol. 124, no. 1, pp. 25–32, Jan. 1998.
- [18] S. Sahin, "An empirical approach for determining longitudinal dispersion coefficients in rivers," *Environ. Process.*, vol. 1, no. 3, pp. 277–285, Sep. 2014.

- [19] R. Noori, Z. Deng, A. Kiaghadi, and F. T. Kachoozangi, "How reliable are ANN, ANFIS, and SVM techniques for predicting longitudinal dispersion coefficient in natural rivers?" *J. Hydraul. Eng.*, vol. 142, no. 1, Jan. 2016, Art. no. 04015039.
- [20] M. J. Alizadeh, A. Shabani, and M. R. Kavianpour, "Predicting longitudinal dispersion coefficient using ANN with Metaheuristic training algorithms," *Int. J. Environ. Sci. Technol.*, vol. 14, no. 11, pp. 2399–2410, Nov. 2017.
- [21] H. Riahi-Madvar, S. A. Ayyoubzadeh, E. Khadangi, and M. M. Ebadzadeh, "An expert system for predicting longitudinal dispersion coefficient in natural streams by using ANFIS," *Expert Syst. Appl.*, vol. 36, no. 4, pp. 8589–8596, May 2009, doi: [10.1016/j.eswa.2008.10.043](https://doi.org/10.1016/j.eswa.2008.10.043).
- [22] J. Elder, "The dispersion of marked fluid in turbulent shear flow," *J. Fluid Mech.* vol. 5, no. 4, pp. 544–560, 1959.
- [23] H. B. Fischer, "The mechanics of dispersion in natural streams," *J. Hydraul. Division*, vol. 93, no. 6, pp. 187–216, 1967.
- [24] A. D. Koussis and J. Rodriguez-Mirasol, "Hydraulic estimation of dispersion coefficient for streams," *J. Hydraul. Eng.*, vol. 124, no. 3, pp. 317–320, Mar. 1998.
- [25] Z.-Q. Deng, V. P. Singh, and L. Bengtsson, "Longitudinal dispersion coefficient in straight rivers," *J. Hydraul. Eng.*, vol. 127, no. 11, pp. 919–927, Nov. 2001.
- [26] Y. Iwasaand and S. Aya, "Predicting longitudinal dispersion coefficient in open-channel flows," in *Proc. Int. Symp. Environ. Hydraul. Hong Kong: Hong Kong Univ. Press*, 1991, pp. 505–510.
- [27] T. Disley, B. Gharabaghi, A. Mahboubi, and E. A. McBean, "Predictive equation for longitudinal dispersion coefficient," *Hydrol. Process.* vol. 29, no. 2, pp. 161–172, 2015.
- [28] R. R. Sahay and S. Dutta, "Prediction of longitudinal dispersion coefficients in natural rivers using genetic algorithm," *Hydrol. Res.*, vol. 40, no. 6, pp. 544–552, Dec. 2009.
- [29] A. Etemad-Shahidi and M. Taghipour, "Predicting longitudinal dispersion coefficient in natural streams using M5' model tree," *J. Hydraul. Eng.*, vol. 138, no. 6, pp. 542–554, Jun. 2012.
- [30] X. Li, H. Liu, and M. Yin, "Differential evolution for prediction of longitudinal dispersion coefficients in natural streams," *Water Resour. Manage.*, vol. 27, pp. 5245–5260, Oct. 2013.
- [31] A. M. A. Sattar and B. Gharabaghi, "Gene expression models for prediction of longitudinal dispersion coefficient in streams," *J. Hydrol.*, vol. 524, pp. 587–596, May 2015.
- [32] M. Atieh, S. L. Mehlretter, B. Gharabaghi, and R. Rudra, "Integrative neural networks model for prediction of sediment rating curve parameters for ungauged basins," *J. Hydrol.*, vol. 531, pp. 1095–1107, Dec. 2015.
- [33] R. Harvey, E. A. McBean, and B. Gharabaghi, "Predicting the timing of water main failure using artificial neural networks," *J. Water Resour. Planning Manage.*, vol. 140, no. 4, pp. 425–434, Apr. 2014.
- [34] M. Dehghani, A. Seifi, and H. Riahi-Madvar, "Novel forecasting models for immediate-short-term to long-term influent flow prediction by combining ANFIS and grey wolf optimization," *J. Hydrol.*, vol. 576, pp. 698–725, Sep. 2019.
- [35] H. Riahi-Madvar and A. Seifi, "Uncertainty analysis in bed load transport prediction of gravel bed rivers by ANN and ANFIS," *Arabian J. Geosci.*, vol. 11, no. 21, p. 688, Nov. 2018.
- [36] A. Seifi and H. Riahi, "Estimating daily reference evapotranspiration using hybrid gamma test-least square support vector machine, gamma test-ANN, and gamma test-ANFIS models in an arid area of iran," *J. Water Climate Change*, vol. 11, no. 1, pp. 217–240, Mar. 2020.
- [37] M. Dehghani, B. Saghafian, F. N. Saleh, A. Farokhnia, and R. Noori, "Uncertainty analysis of streamflow drought forecast using artificial neural networks and Monte-Carlo simulation," *Int. J. Climatol.*, vol. 34, no. 4, pp. 1169–1180, Mar. 2014.
- [38] O. Kisi, O. Genc, S. Dinc, and M. Zounemat-Kermani, "Daily pan evaporation modeling using chi-squared automatic interaction detector, neural networks, classification and regression tree," *Comput. Electron. Agricult.*, vol. 122, pp. 112–117, Mar. 2016.
- [39] M. Dehghani, B. Saghafian, F. Rivaz, and A. Khodadadi, "Evaluation of dynamic regression and artificial neural networks models for real-time hydrological drought forecasting," *Arabian J. Geosci.*, vol. 10, no. 12, Jun. 2017.
- [40] R. Prasad, R. C. Deo, Y. Li, and T. Maraseni, "Input selection and performance optimization of ANN-based streamflow forecasts in the drought-prone murray darling basin region using IIS and MODWT algorithm," *Atmos. Res.*, vol. 197, pp. 42–63, Nov. 2017.
- [41] Y. W. Soh, C. H. Koo, Y. F. Huang, and K. F. Fung, "Application of artificial intelligence models for the prediction of standardized precipitation evapotranspiration index (SPEI) at Langat River Basin, Malaysia," *Comput. Electron. Agricult.*, vol. 144, pp. 164–173, Jan. 2018.
- [42] N. Nabipour, M. Dehghani, A. Mosavi, and S. Shamshirband, "Short-term hydrological drought forecasting based on different nature-inspired optimization algorithms hybridized with artificial neural networks," *IEEE Access*, vol. 8, pp. 15210–15222, 2020.
- [43] F. Saberi-Movahed, M. Najafzadeh, and A. Mehrpooya, "Receiving more accurate predictions for longitudinal dispersion coefficients in water pipelines: Training group method of data handling using extreme learning machine conceptions," *Water Resour. Manage.*, vol. 34, no. 2, pp. 529–561, Jan. 2020.
- [44] M. Najafzadeh and A. Tafarjoruz, "Evaluation of neuro-fuzzy GMDH-based particle swarm optimization to predict longitudinal dispersion coefficient in rivers," *Environ. Earth Sci.*, vol. 75, no. 2, p. 157, Jan. 2016.
- [45] H. M. Azamathulla and A. A. Ghani, "Genetic programming for predicting longitudinal dispersion coefficients in streams," *Water Resour. Manage.*, vol. 25, no. 6, pp. 1537–1544, Apr. 2011.
- [46] R. R. Sahay, "Predicting longitudinal dispersion coefficients in sinuous rivers by genetic algorithm," *J. Hydrol. Hydromech.*, vol. 61, no. 3, pp. 214–221, 2013.
- [47] A. P. Piotrowski, P. M. Rowinski, and J. J. Napiorkowski, "Comparison of evolutionary computation techniques for noise injected neural network training to estimate longitudinal dispersion coefficients in rivers," *Expert Syst. Appl.*, vol. 39, no. 1, pp. 1354–1361, Jan. 2012.
- [48] A. M. A. Sattar, "Gene expression models for the prediction of longitudinal dispersion coefficients in transitional and turbulent pipe flow," *J. Pipeline Syst. Eng. Pract.*, vol. 5, no. 1, Feb. 2014, Art. no. 04013011.
- [49] S.-C. Chu and P.-W. Tsai, "Computational intelligence based on the behavior of cats," *Int. J. Innov. Comput., Inf. Control*, vol. 3, no. 1, pp. 163–173, 2007.
- [50] J. Guo, Z. Sun, H. Tang, L. Yin, and Z. Zhang, "Improved cat swarm optimization algorithm for assembly sequence planning," *Open Autom. Control Syst. J.*, vol. 7, no. 1, pp. 792–799, Aug. 2015.
- [51] O. Bozorg-Haddad, Ed., *Advanced Optimization by Nature-Inspired Algorithms*. Singapore: Springer, 2017.
- [52] P.-W. Tsai and V. Istanda, "Review on cat swarm optimization algorithms," in *Proc. 3rd Int. Conf. Consum. Electron., Commun. Netw.*, Nov. 2013, pp. 564–567.
- [53] M. Clerc and J. Kennedy, "The particle swarm—explosion, stability, and convergence in a multidimensional complex space," *IEEE Trans. Evol. Comput.*, vol. 6, no. 1, pp. 58–73, Feb. 2002.
- [54] M. Siavashi and M. H. Doranehgard, "Particle swarm optimization of thermal enhanced oil recovery from oilfields with temperature control," *Appl. Thermal Eng.*, vol. 123, pp. 658–669, Aug. 2017.
- [55] M. Fereidoon and M. Koch, "SWAT-MODSIM-PSO optimization of multi-crop planning in the Karkheh River Basin, Iran, under the impacts of climate change," *Sci. Total Environ.*, vol. 630, pp. 502–516, Jul. 2018.
- [56] W. Roberts, G. P. Williams, E. Jackson, E. J. Nelson, and D. P. Ames, "Hydrostats: A Python package for characterizing errors between observed and predicted time series," *Hydrology*, vol. 5, no. 4, p. 66, Dec. 2018, doi: [10.3390/hydrology5040066](https://doi.org/10.3390/hydrology5040066).
- [57] E. K. Jackson, W. Roberts, B. Nelsen, G. P. Williams, E. J. Nelson, and D. P. Ames, "Introductory overview: Error metrics for hydrologic modelling—A review of common practices and an open source library to facilitate use and adoption," *Environ. Model. Softw.*, vol. 119, pp. 32–48, Sep. 2019, doi: [10.1016/j.envsoft.2019.05.001](https://doi.org/10.1016/j.envsoft.2019.05.001).
- [58] M. Zeynoddin, H. Bonakdari, A. Azari, I. Ebtehaj, B. Gharabaghi, and H. R. Madavar, "Novel hybrid linear stochastic with non-linear extreme learning machine methods for forecasting monthly rainfall a tropical climate," *J. Environ. Manage.*, vol. 222, pp. 190–206, Sep. 2018.
- [59] I. Ebtehaj, H. Bonakdari, M. J. S. Safari, B. Gharabaghi, A. H. Zaji, H. R. Madavar, Z. S. Khozani, M. S. Es-Haghi, A. Shishegaran, and A. D. Mehr, "Combination of sensitivity and uncertainty analyses for sediment transport modeling in sewer pipes," *Int. J. Sediment Res.*, vol. 35, no. 2, pp. 157–170, Apr. 2020.
- [60] A. Seifi and F. Soroush, "Pan evaporation estimation and derivation of explicit optimized equations by novel hybrid meta-heuristic ANN based methods in different climates of iran," *Comput. Electron. Agricult.*, vol. 173, Jun. 2020, Art. no. 105418, doi: [10.1016/j.compag.2020.105418](https://doi.org/10.1016/j.compag.2020.105418).

...